Smart Structures and Systems, *Vol. 33, No. 2 (2024) 133-143*
https://doi.org/10.12989/sss.2024.33.2.133

Study of nonlinear hysteretic modelling and performance evaluation for piezoelectric actuators based on activation functions

Xingyang Xie [1,2], Yuguo Cui[*1] and Yang Yu[**3]

[1] *Faculty of Mechanical Engineering & Mechanics, Ningbo University, Ningbo, Zhejiang, China*
[2] *Taizhou Customs Comprehensive Technical Service Center, Taizhou, Zhejiang, China*
[3] *Centre for Infrastructure Engineering and Safety, School of Civil and Environmental Engineering, The University of New South Wales, Sydney, NSW 2052, Australia*

(*Received December 12, 2022, Revised December 27, 2023, Accepted January 9, 2024*)

Abstract. Piezoelectric (PZT) actuators have been widely used in precision positioning fields for their excellent displacement resolution. However, due to the inherent characteristics of piezoelectric actuators, hysteresis has been proven to greatly reduce positioning performance. In this paper, five mathematical hysteretic models based on activation function are proposed to characterize the nonlinear hysteresis characteristics of piezoelectric actuators. Then the performance of the proposed models is verified by particle swarm optimization (PSO) algorithm and the experiment data. Thirdly, the fitting performance of the proposed models is compared with the classical Bouc-Wen model. Finally, the performance of the five proposed models in modelling hysteresis nonlinearity of piezoelectric drivers is compared, in terms of RMSE, MAPE, SAPE and operation efficiency, and relevant suggestions are given.

Keywords: activation function; hysteresis modelling; particle swarm optimization (PSO) algorithm; piezoelectric actuators

1. Introduction

Piezoelectric (PZT) actuators are micro-actuators that use the inverse piezoelectric effect of piezoelectric materials. With the advantages of small size, high resolution and fast response speed, they have become important positioning and driving components in precision positioning systems. PZT actuators are widely used in scanning probe microscopy (Kenton *et al*. 2011, Vorbringer-Dorozhovets *et al*. 2011), micro-nano operation (Kim *et al*. 2004, Ionescu *et al*. 2011), semiconductor processing (Jung and Huh 2010, Liu *et al*. 2010, Tue *et al*. 2019) aerospace application (Ali *et al*. 2019, Sherrit *et al*. 2011, Sente *et al*. 2011). However, piezoelectric material has obvious nonlinear hysteresis characteristics, and the corresponding boost and depressurize curves of piezoelectric material do not coincide, resulting in an error in positioning. For example, a driver made of a certain piezoelectric material will produce a hysteresis error of up to 10% - 15% (Tao and Kokotovic 1995). This will decrease the control accuracy and stability of the system, and even produce system turbulence. In many fields, how to eliminate the hysteresis effect on positioning and realize the effective control of piezoelectric actuator has become a key point in the research of precision positioning control.

There are mainly two ways to minimize the hysteresis effect on position: feedback control and open-loop control. Feedback control can reduce errors and achieve high accuracy in many PZT application devices. However, due to space limitation, sensors can't be installed in some experimental places to realize closed-loop feedback control. So the open-loop control method based on high model accuracy seems to be a more feasible way. In order to accurately position and control PZT actuators, it is necessary to establish a model that can accurately simulate the hysteresis effect of PZT actuators. The earliest modelling method is to give the whole limit curve in the form of parameter table, but the accuracy is very low, so a more complex mathematical hysteresis model is used to fit the hysteresis curve of PZT actuators.

In the past few years, studies have been conducted to develop the hysteresis models for PZT actuators. In general, related models are categorised into two groups: physical models (Guo *et al*. 2014, Schweizer 2017) and phenomenological models (Luo *et al*. 2019, Nguyen *et al*. 2018). Physical hysteresis models are hard to build because of complicated physics of real systems with nonlinear hysteresis. Then, phenomenological hysteresis models become a more feasible way.

Different from physical models, phenomenological hysteresis models employ numerical equations directly instead of the natural physical properties. Accordingly, several phenomenological models have been developed, such as Preisach model (Pasco and Berry 2004, Xiao and Li 2012), Maxwell slip model (Liu *et al*. 2021, Liu *et al*.

*Corresponding author, Ph.D.,
E-mail: cuiyuguo@nbu.edu.cn
**Co-corresponding author, Ph.D.,
E-mail: yang.yu12@unsw.edu.au

ISSN: 1738-1584 (Print), 1738-1991 (Online)

2019), randtl-Ishlinskii model (Feng and Li 2021, Savoie and Shan 2022), Dahl model (Xu and Li 2010), Duhem model (Gan and Zhang 2019, Ji *et al*. 2022), Bouc-Wen (BW) model (Zhang *et al*. 2019, Gan and Zhang 2019, Wang and Zhu 2011) etc.

The models above have found application in many fields. Preisach model (Mittal and Meng 2000, Nguyen *et al*. 2018, Pasco and Berry 2004), Generalized Maxwell-Slip (GMS) model (Liu *et al*. 2020, 2021), Prandtl-Ishlinskii (PI) model (Al Janaideh *et al*. 2016, Rakotondrabe 2017, Savoie and Shan 2022), Rayleigh model (Zhang and Damjanovic 2020), Dahl model (Shome *et al*. 2018), Dieng model (Gan and Zhang 2019, Ji *et al*. 2022, Li *et al*. 2022), Bouc-Wen (BW) model (Qian *et al*. 2020) are widely used in nonlinear hysteresis modeling of piezoelectric actuators. Liu *et al*. (2020) proposed an adaptive generalized Maxwell-slip (AGMS) algorithm to identify and compensate for hysteresis online. Savoie and Shan (2022) introduced asymmetry and temperature dependence into PI model, and established a temperature-dependent asymmetric Prandtl-Ishlinskii (TAPI) model to describe the change of the displacement curve of piezoelectric actuator (PEA) with temperature. Gan and Zhang (2019) introduced trigonometric functions and proposed an improved Duhem model (MDM). Zhang and Damjanovic (2020) proposed a quasi-Rayleigh model to describe the hysteresis behavior of PEAs and piezo-based systems. The method is based on two modified Rayleigh parameters and their corresponding coefficients, which are used to describe the ascending and descending curves of hysteresis trajectory. In addition, as classical friction models, LuGre friction model and LeuVen model have also been reported for hysteresis modeling of piezoelectric actuators (Fung *et al*. 2008).

The models above have their own advantages. For example, the GMS model improves the simulation accuracy of hysteresis curves by increasing the number of elastic slide elements. Prandtl-Ishlinskii model is widely used in hysteresis modeling of intelligent actuators because of its advantage of analytic inverse model. Through selecting appropriate undetermined parameters, the Bouc-Wen model is widely used in the simulation of hysteresis of magnetorheological damps, structural science, isolation devices and soil behavior (Huang *et al*. 2019). However, there are still some problems in the models above, such as too many model parameters, difficult identifying parameters, high simulation error, and not easy to solve nonlinear differential equation. For example, the Bouc-Wen model has many parameters, and highly nonlinear differential equations in the expression are also a challenging problem to deal with.

Based on the analysis above, an ideal hysteresis model of PZT actuators should achieve high precision and easy identification, while avoiding too many parameters and being difficult to solve. Activation functions are mostly piece-wise linear or nonlinear exponential functions, and feature S-shaped curve characteristics. By its own nonlinear phenomenological characteristics, it can effectively avoid the drawbacks of nonlinear equations and too many parameters, then can play an important role in realizing the nonlinear mapping of input features. This feature can increase the non-linearity of the neural network model. In this paper, the S-shaped curve of the activation function is utilized for nonlinear fitting of the hysteresis loop of the piezoelectric actuators, featuring fewer adjustable parameters and no highly nonlinear differential equations in the expression. Five activation functions are introduced and integrated into mathematical models to describe the nonlinear hysteresis displacement-voltage response of piezoelectric actuators. Based on the PSO algorithm, the model parameters are identified, and the experimental data of piezoelectric drivers under different load frequencies and voltages are used to verify the proposed five hysteresis models. The superiority of the five proposed models to the classical Bouc-Wen model is also proven. Finally, in order to better perform the modeling of piezoelectric actuators, the performance among the five proposed hysteresis models is compared, and relative suggestion is recommended.

In this pater, Particle swarm optimization (PSO) is employed to evaluate the performance of the proposed models. PSO algorithm is based on population theory that is used to simulate the social behaviors like bird flocking, fish schooling, and wasp swarming. By continually updating the exploring information of each particle, the PSO is regarded as an effective way to search the optimal solution at a limited iteration number (Yu *et al*. 2015). Similar to bird flocking, all the particles are allocated with different velocities which guide them to fly through the solution domain. At the same time, the optimal solutions obtained by both the individual and the whole swarm are recorded and utilized as the guidance for the following searching. The optimal solution is finally obtained when the searching process satisfies some stopping criterion. The PSO algorithm has the advantages of fast convergence speed, few parameters, simple algorithm and easy implementation. For high dimensional optimization problems, it converges to the optimal solution faster than genetic algorithm. Some studies (Baziyad *et al*. 2022, Ali *et al*. 2010, Muftah *et al*. 2022, Aziz *et al*. 2018) have proven that the effectiveness of PSO algorithm in various fields, including piezoelectric area. The procedure of PSO algorithm is to resolve a globally minimal optimisation problem (Nguyen *et al*. 2021, Tang *et al* 2013, Das and Dhang 2020). In summary, PSO algorithm can be an effective way to simulate hysteresis characteristics of PZT actuators.

2. Phenomenological hysteresis model based on activation function

2.1 Activation function

Activation functions are piece-wise linear or exponential nonlinear functions, which can effectively increase the non-linearity of neural network models. Five activation functions are selected in this paper, shown in the Eq. (1).

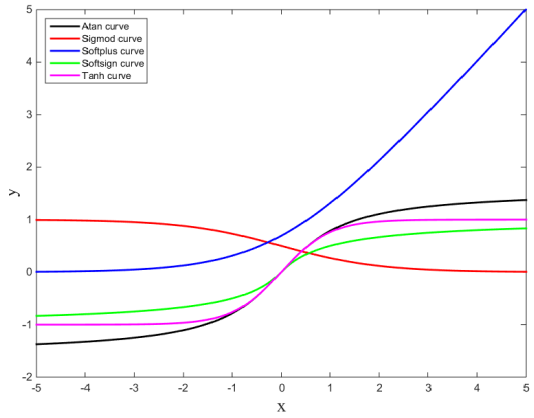

Fig. 1 Curves of activation function

$$f_i(x) = \begin{cases} \text{atan}(\gamma u(t)) & when\ i = 1 \\ \dfrac{1}{1+\exp(-\gamma u(t))} & when\ i = 2 \\ \ln(1+\exp(\gamma u(t))) & when\ i = 3 \\ \dfrac{\gamma u(t)}{1+|\gamma u(t)|} & when\ i = 4 \\ \tanh(\gamma u(t)) & when\ i = 5 \end{cases} \quad (1)$$

Among the equation, $f_2(x) = \frac{1}{1+\exp(-\gamma u(t))}$ is called Sigmoid function, $f_3(x) = \ln(1+\exp(\gamma u(t)))$ is called Softplus function, $f_4(x) = \frac{\gamma u(t)}{1+|\gamma u(t)|}$ is called Softsign function, $f_5(x) = \tanh(\gamma u(t))$ is called Hyperbolic tangent function.

The following figure shows the plots of the five activation functions above in range [-5,5], which are inverse tangent function, Softplus function, Sigmoid function, Softsign function and hyperbolic tangent function in turn. As can be seen from the figure, the five functions have obvious nonlinear characteristics and resemble the letter S. The performance of fitting nonlinear hysteretic characteristics of PZT actuator based on activation functions above will be elaborated in detail below.

2.2 Phenomenological hysteresis model based on activation function

Five efficient hysteresis models based on activation functions are proposed, and their expressions are shown in Eq. (2).

$$z_h(t) = k_0 u(t) + \alpha \dot{u}(t) + \beta f_i(x)$$
$$f_i(x) = \begin{cases} \text{atan}(\gamma u(t)) & when\ i = 1 \\ \dfrac{1}{1+\exp(-\gamma u(t))} & when\ i = 2 \\ \ln(1+\exp(\gamma u(t))) & when\ i = 3 \\ \dfrac{\gamma u(t)}{1+|\gamma u(t)|} & when\ i = 4 \\ \tanh(\gamma u(t)) & when\ i = 5 \end{cases} \quad (2)$$

Where $z_h(t)$ represents the hysteresis displacement output, $u(t)$ is the input voltage, k_0 is a parameter to represent the stiffness of system, α represents viscosity coefficient of system, and the parameters of β and γ are related to the shape of hysteresis loops. Among the equation, $k_0 u(t)$ determines the Max/Min displacement output of piezoelectric actuators, $\alpha\dot{u}(t)$ determines the size of hysteresis loop, $\beta \cdot f_i(x)$ determines the fundamental hysteresis loop.

Obviously, the five proposed models in this study use elements based on inverse Tangent function, Sigmoid function, Softplus function, Softsign function and Hyperbolic tangent function, respectively, to characterize the nonlinear characteristics of displacement-voltage, with the advantages of less undetermined parameters and no highly differential equation.

2.3 Analysis of the parameters in the proposed models

In this paper, the influence of different model parameters on displacement output is numerically studied. Considering the first two items of the equation are the same and only $f_i(x)$ makes the difference in the five proposed models, $f_5(x) = \tanh(\gamma u(t))$ is determined as the precondition while observing the influence of k_0, α, β on displacement.

The model reference parameter is set as: k_0 = 0.145, α = -0.0001, β = 0.385. Then harmonic wave voltage is exerted on PZT actuators, shown as Eq. (3)

$$u(t) = V_a \cdot \sin(2\pi f_v t + \varphi_0) + V_a \quad (3)$$

Where, V_a is the input voltage; f_v denotes the excitation frequency; φ_0 is the initial phase angle of voltage excitation. In this investigation, V_a, f_v and φ_0 are set to 40 V, 10 Hz and -π/2, respectively. The sampling frequency and duration are set to 1000 Hz and 0.05 s, so a complete cycle of data can be obtained for this numerical analysis.

Then, each model parameter changes in a certain range from the reference value, while other parameters are set as reference values. Fig. 2 portrays the hysteretic loops of the proposed model with different combinations of model parameters. Fig. 2(a) shows the displacement outputs corresponding to different values of k_0 of 0.0435, 0.087, 0.1305, 0.174 and 0.2175, respectively. Obviously, the maximum displacement output increases linearly with increasing k_0, because it represents the stiffness of the system and is related to the slope of the hysteresis loop. The influence of α on the hysteresis loop is shown in Fig. 2(b). Unlike k_0, the change of α, which represents the viscosity capacity of the system, doesn't affect the minimum and maximum displacement outputs. With the increase of α value, the closed area expands and the energy dissipation capacity increases. Fig. 2(c) depicts the hysteresis at different beta values. It can be seen that β has little effect on the shape of the response, including the width and shape of the hysteresis loop. And β is proportional to the magnitude of the output displacement. The larger the β is, the larger the displacement becomes.

Then, k_0, α, β are set to k_0 = 0.145, α = -0.0001,

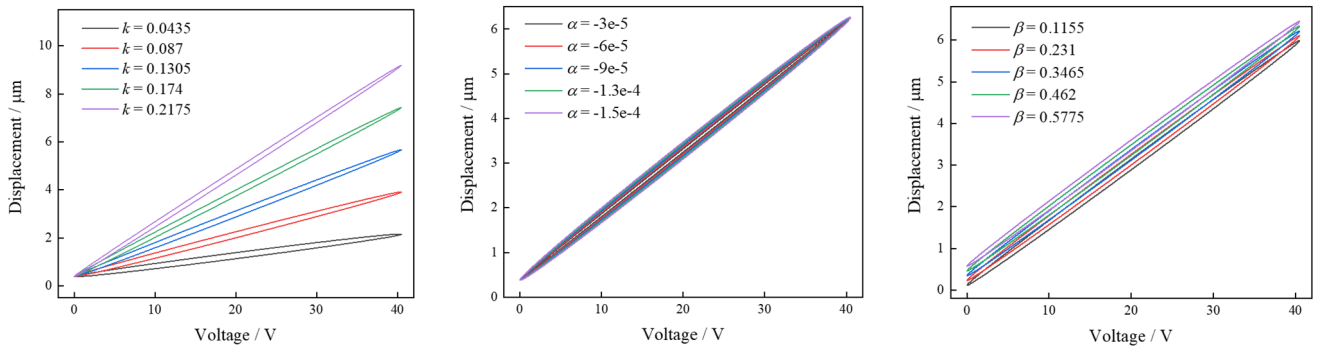

(a) k_0 (b) α (c) β

Fig. 2 Influences of model parameters (k_0, α, β) on displacement outputs

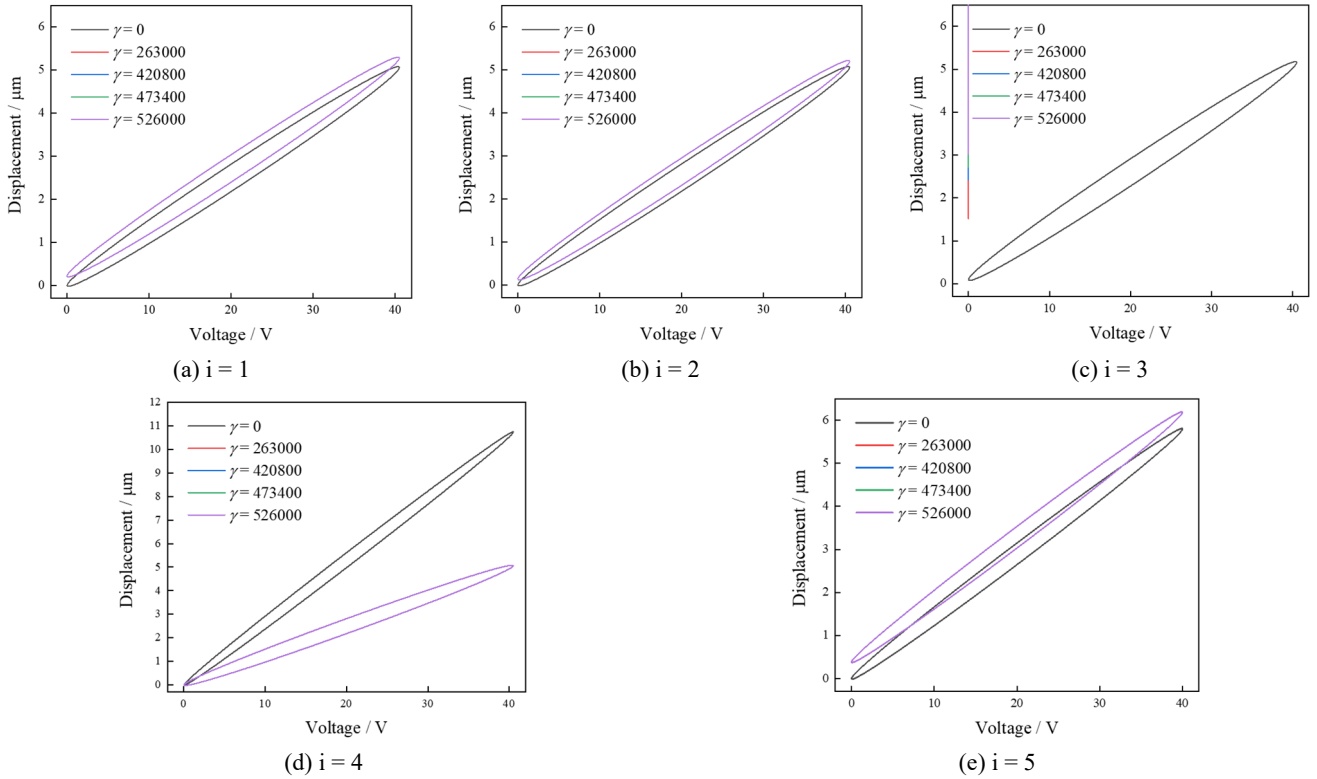

(a) i = 1 (b) i = 2 (c) i = 3

(d) i = 4 (e) i = 5

Fig. 3 Influences of model parameter (γ) on displacement outputs

β = 0.385, respectively. And γ is changed to observe its influence on the displacement hysteresis loop. The range of variation is 0, 50%, 80%, 90% and 100% of the corresponding reference value of 526000. Fig. 3 illustrates the effect of γ on displacement output. It can be seen from the analysis results that only one curve can be observed in the hysteresis model with Softplus function, and only two curves can be seen in the hysteresis model with the four other activation functions. The main reason for this result is that when the absolute value of γ is greater than a certain value, the activation function reaches the upper and lower limits, respectively.

3. Modelling verification

3.1 Experimental measurements of PZT displacement

The experimental setup for displacement measurement of PZT actuator is shown in Fig. 4. The experimental system consists of a computer, multifunctional data acquisition (DAQ) board card, PZT ceramic drive power supply, PZT actuator, drive unit, capacitive displacement sensor, auxiliary measurement bracket and 3D manual fine-tuning table. The measurement process is provided as follows: The multi-function (DAQ) board card converts the digital signal output by the computer into analog signal, which is output to the piezoelectric ceramic drive power supply. The output voltage of the drive power supply acts

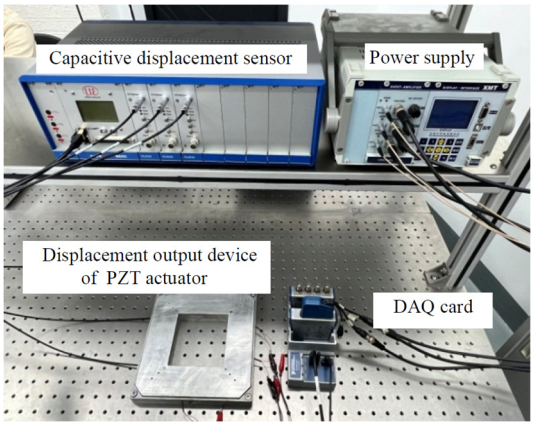

Fig. 4 Displacement measurement system of PZT

Table 1 Model and main parameters of the equipments

Equipment	Model	Resolution	Bandwidth/ Sampling rate
Piezoelectric driver	XE501-C	16 bit	0~2000 Hz
DAQ	NI 9263	16 bit	100 kS/s/ch
Capacitive sensor	CSE1	1 nm	N/A

on the PZT actuator, and the drive unit produces micro displacement. The displacement can be measured by the capacitive displacement sensor, and finally the measured displacement is collected into the computer through the network port.

Table 1 gives the instrument models and main parameters used in the experimental test system. Sine wave voltages of 0-20-0 V, 0-40-0 V and 0-60-0 V are applied to the PZT actuators in the driving unit, respectively. The frequency changes in the range of 10 Hz ~ 80 Hz, with each increase of 10 Hz every time. The displacement output results are tested repeatedly. Then the hysteresis relation between output displacement and input voltage is obtained. In order to obtain stable results, the sampling time of all tests is five excitation cycles. The displacement and voltage values can be obtained directly from the sensor readings, while the rate of voltage change can be calculated by differentiating the time and voltage response.

3.2 Identification of model parameters

The procedure of PSO algorithm is to resolve a globally minimal optimisation problem. The key to the optimisation problem is to define a reasonable objective function, also known as fitness function. Here, the root means square error (RMSE) between measured displacements and model predicted values in one sampling cycle is employed as the optimisation target, with the mathematical formulation shown as follows.

$$RMSE = \frac{1}{N_{oc}}\sum_{t=1}^{N_{oc}}\left[z_h^{pred}(t) - z_h^{exp}(t)\right]^2 = \frac{1}{N_{oc}}\sum_{t=1}^{N_{oc}}\left[k_0 u(t) + \alpha\dot{u}(t) + \beta \cdot f_i(x) - z_h^{exp}(t)\right]^2 \quad (4)$$

where N_{oc} denotes the sample number in one sampling frequency. For different excitation frequencies, the values of N_{oc} are different. z_h^{exp} and z_h^{pre} are experimentally measured displacement and predicted displacement by the proposed model, respectively. Using PSO algorithm to resolve the fitness function is an iterative procedure, the model parameters of k_0, α, β and γ are constantly updated to lower the RMSE value as small as possible. If the fitness value is close to 0, the corresponding solution is the optimal values of model parameters. Accordingly, the model parameter optimisation problem can be formulated as

$$\text{Min } RMSE(k_0, \alpha, \beta, \gamma) \quad (5)$$

Since there are eight frequencies and three input voltage levels, a total of 24 groups of parameter combinations need to be identified using the PSO algorithm. The implementation of PSO is based on Matlab v2016a optimization toolbox. The parameter setting of PSO is given as follows: The swarm size is 30, the maximum iteration number is 200, and the inertia weight factor and learning factor are 0.8 and 1.5, respectively.

To shorten the representation space of simulation results, only identification results under 0-40-0 V are given in this paper. The identification results are summarized in Tables 2-6.

Table 2 Identification results of the proposed model (i = 1) parameters under the loading voltage case of 0-40-0 V

Frequency	k_0	α	β	γ
10 Hz	0.1516	-0.00017	0.1996	1000
20 Hz	0.1487	-0.00016	0.2211	1000
30 Hz	0.1481	-0.000063	0.2149	1000
40 Hz	0.1456	-0.000093	0.2564	541.3729
50 Hz	0.1441	-0.000092	0.2673	532.2059
60 Hz	0.1422	-0.0001	0.2725	1000
70 Hz	0.1396	-0.000104	0.3107	1000
80 Hz	0.1445	-0.000028	0.2669	522.4845

Table 3 Identification results of the proposed model (i = 2) parameters under the loading voltage case of 0-40-0 V

Frequency	k_0	α	β	γ
10 Hz	0.1516	-0.00017	0.3131	1000
20 Hz	0.1483	-0.00016	0.6891	0.0028
30 Hz	0.1482	-0.000006	0.336	1000
40 Hz	0.1461	-0.000093	0.3851	997.9669
50 Hz	0.1445	-0.000092	0.4068	541.3878
60 Hz	0.1422	-0.0001	0.429	552.4445
70 Hz	0.1397	-0.0001	0.4849	1000
80 Hz	0.1432	-0.000028	0.4608	499.6622

Table 4 Identification results of the proposed model (i = 2) parameters under the loading voltage case of 0-40-0 V

Frequency	k_0	α	β	γ
10 Hz	0.1411	-0.00017	0.4503	0.0342
20 Hz	0.1121	-0.00016	0.5849	0.0782
30 Hz	0.1482	-0.000063	0.4831	0.0369
40 Hz	0.1369	-0.000093	0.5637	0.0265
50 Hz	0.1342	-0.000092	0.5948	0.0278
60 Hz	0.1331	-0.0001	0.6232	0.0242
70 Hz	0.1397	-0.0001	0.6965	0.0234
80 Hz	0.089	-0.000028	0.7053	0.0957

Table 5 Identification results of the proposed model (i = 4) parameters under the loading voltage case of 0-40-0 V

Frequency	k_0	α	β	γ
10 Hz	0.1516	-0.00017	100	318.2799
20 Hz	0.1486	-0.00016	99.9999	286.9318
30 Hz	0.1481	-0.000063	100	295.5721
40 Hz	0.146	-0.000092	100	257.9082
50 Hz	0.1445	-0.000092	100	245.9069
60 Hz	0.1422	-0.0001	100	232.9167
70 Hz	0.1395	-0.0001	100	204.1493
80 Hz	0.1449	-0.000028	100	246.3472

Table 6 Identification results of the proposed model (i = 5) parameters under the loading voltage case of 0-40-0 V

Frequency	k_0	α	β	γ
10 Hz	0.1517	-0.00017	0.3121	113971
20 Hz	0.1487	-0.00016	0.3454	976595
30 Hz	0.1482	-0.00006	0.3349	499290
40 Hz	0.1461	-0.00009	0.3857	500032
50 Hz	0.1447	-0.00009	0.4017	54236
60 Hz	0.1424	-0.00010	0.4234	888161
70 Hz	0.1397	-0.00010	0.4828	988761
80 Hz	0.1451	-0.00003	0.4004	187906

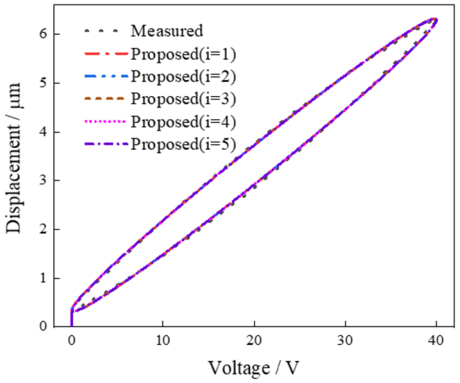

(a) 20 Hz

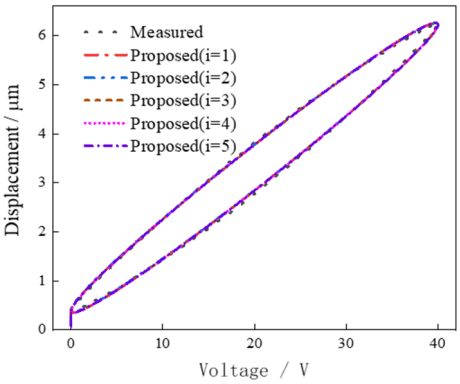

(b) 40 Hz

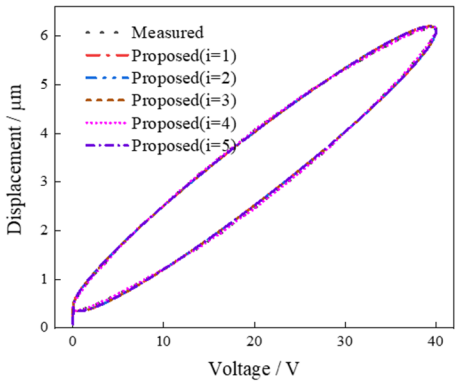

(c) 60 Hz

Fig. 5 Simulation and experimental fitting diagram of the five proposed models under 0-40-0 V

3.3 Verification of the five proposed Models

Fig. 5 compares the hysteresis responses predicted by the five proposed models under the loading conditions of 20 Hz, 40 Hz and 60 Hz at 0-40-0 V voltage. The results show that with the increase in excitation frequency, the hysteresis loop width increases, but the maximum displacement output does not change. The perfect match between the measured displacement and the predicted displacement verifies the ability of the five proposed hysteresis models to characterize the displacement-voltage responses of PZT actuators. It is worth noting that the mean absolute error of all cases is very low, representing a high prediction accuracy. When the frequency is 20 Hz, the absolute error distribution between the actual displacement and the predicted displacement is in the range of -0.2 to 0.2 μm. At the frequency of 40 Hz, the absolute error is in the range of -0.15 to 0.15 μm. At the frequency of 60 Hz, the absolute error between the actual displacement and the predicted displacement is between -0.12 and 0.12 μm. In general, the prediction error is acceptable in the modeling study.

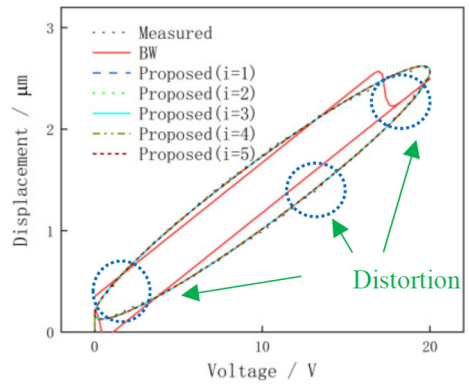

(a) 0-20-0 V

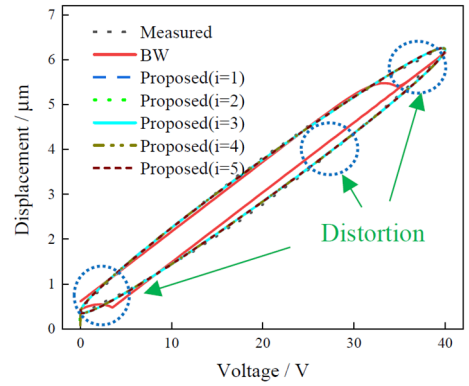

(b) 0-40-0 V

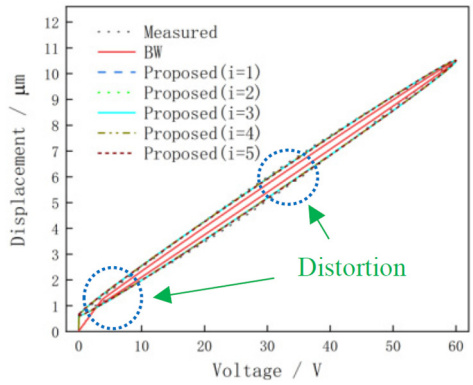

(c) 0-60-0 V

Fig. 6 Simulation and experimental fitting diagram of the five proposed models under 40 Hz

4. Performance study

4.1 Comparison between the five proposed models and Bouc-wen model

To demonstrate the superiority of the proposed models over existing models in depicting the hysteresis responses of PZT actuators, a comparative study is conducted by comparison with commonly used BW model. Due to its excellent simulation ability, Bouc-wen model has been widely used in nonlinear hysteresis simulation of PZT actuators. Bouc-wen model adopts a nonlinear differential equation with specific parameters to simulate hysteresis, as shown in Eqs. (6)-(7). As shown in Eqs. (6)-(7), k_0 denote the stiffness coefficient, α, β, γ and n are nondimensional parameters that regulate the size and shape of the hysteretic loop. Among the parameters, α control the size of the hysteresis ring, β and γ control the shape of the hysteresis ring, and parameter n controls the sharpness of the hysteresis displacement output $z_h(t)$. The detailed correction is presented as follows. By selecting appropriate undetermined parameters, hysteresis rings of various shapes and types can be obtained, which can simulate different hysteresis behaviors.

$$z_h(t) = k_0 u(t) + g(t) \tag{6}$$

$$\dot{g}(t) = \alpha\dot{u}(t) - \beta|\dot{u}(t)||g(t)|^{n-1}g(t) - \gamma\dot{u}(t)|g(t)|^n \tag{7}$$

Fig. 6 shows an example of performance comparison between the five proposed models and BW model in predicting the displacement-voltage hysteresis effect of PZT actuators when the excitation frequency is set to 40 Hz, with input voltages namely 0-20-0 V, 0-40-0 V and 0-60-0 V respectively. As can be seen from the results in Fig.6, the response curve predicted by the BW model is distorted due to the existence of nonlinear differential equations (highlighted in the figure). In addition, when the input voltage is 0-20-0 V and 0-60-0 V, respectively, the BW model has obvious distortion and even can't close the hysteresis loop when the voltage gets close to 0. However, the hysteresis loops described by the five proposed hysteresis models are very smooth and more consistent with the actual experiments. It can be seen that the five proposed hysteresis models have better fitting performance than the BW model.

To further elaborate the performance of the five proposed models, fitting error comparison is studied. Fig. 7 shows the fitting error curve of the five proposed models and BW model. It can be seen that the fitting errors of BW model are all significantly higher than those of the five proposed models mentioned in this paper, and the error curves of BW model show an irregular trend. Especially under the excitation voltage of 0-40-0 V, the error curve of BW model is up to 0.6 μm, which is much higher than the error of the five proposed models in this paper. In conclusion, the stability and accuracy of the five proposed hysteresis models proposed in this paper are better than that of BW model.

On the analysis above, the five proposed models based on the activation function are superior to the Bouc-Wen model in modelling the nonlinear hysteresis displacement-voltage responses, in terms of the smoothness of hysteresis loops and fitting error.

4.2 Comparison of the five proposed models

To further compare the difference and superiority among the five proposed models, several commonly used statistical metrics are employed to comprehensively compare the performance of the five proposed models. Besides RMSE shown in Eq. (4), mean absolute percentage error (MAPE) and symmetric mean absolute percentage error (SMAPE) are also adopted in the model performance evaluation. For all three metrics, the lower the values of evaluation metrics, the better the model performance. The mathematical

expressions of MAPE and SMAPE are given in Eq. (8) and Eq. (9).

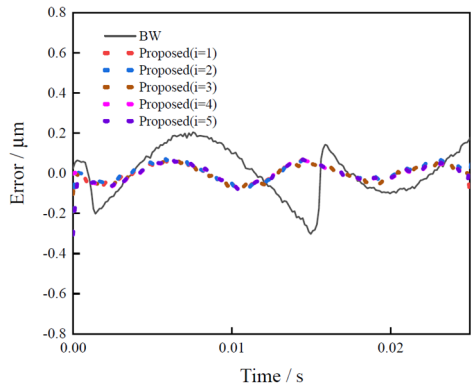

(a) Comparison of error curves under 0-20-0 V

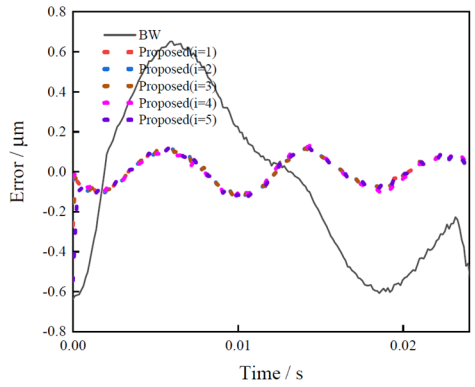

(b) Comparison of error curves under 0-40-0 V

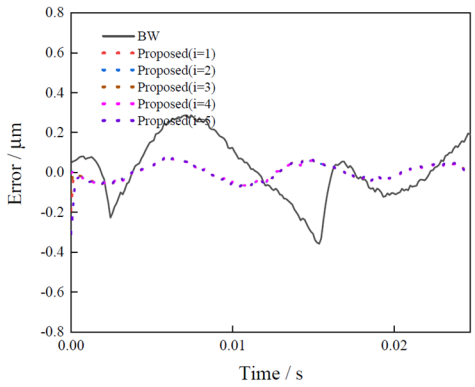

(c) Comparison of error curves under 0-60-0 V

Fig. 7 Error curves of the five proposed models and BW model under 40 Hz

$$MAPE = \frac{1}{N_{oc}} \sum_{t=1}^{N_{oc}} \left| \frac{z_h^{pred}(t) - z_h^{exp}(t)}{z_h^{exp}(t)} \right| \tag{8}$$

$$SMAPE = \frac{1}{N_{oc}} \sum_{t=1}^{N_{oc}} \frac{\left| z_h^{pred}(t) - z_h^{exp}(t) \right|}{(z_h^{pred}(t) + z_h^{exp}(t))/2} \tag{9}$$

To shorten representation space of comparison results, only performance evaluation of RMSE, MAPE and SMAPE under frequencies of 20, 40, 60 and 80 Hz, with voltage respectively 0-20-0 V, 0-40-0 V, 0-60-0 V, are given in this paper. The performance comparison results of the five proposed models are shown in Figs. 8-11 in the form of column map. As can be seen from Figures, under 20 Hz, the five proposed models don't make much difference in terms of RMSE/SMAPE/MAPE. While under 0-20-0 V & 40 Hz case, as can be seen from Fig. 9(a), the proposed model with Atan function (i = 1) records the worst performance among the five proposed models, and the RMSE/SMAPE/MAPE is 0.0843, 0.2088 and 0.3935 respectively, 459.81%, 867.96% and 1657.99% higher than the lowest values in the other four proposed models. The performance also shows that when the excitation level is 0-40-0 V under 50 Hz, the values of RMSE, MAPE and SMAPE of the proposed model with Tanh function (i = 5) are 0.128, 0.1052 and 0.0924, 245.63%, 439.19% and 369.9% higher than the lowest values in the other four proposed models. The proposed model with Softplus function (i = 3) also records the worst under 0-60-0 V, 60 Hz case (see Fig. 10(c)), and the values of RMSE, MAPE and SMAPE are 0.3844, 0.193 and 0.2881, 452.92%, 762.43% and 1165.74% higher than the lowest values in the other four proposed models. The proposed model with Sigmoid function (i = 2) performs badly under 0-20-0 V with frequencies, namely 70 Hz, and 80 Hz. And the values of RMSE, MAPE and SMAPE are 0.0628, 0.1341, 0.1116 and 0.0584, 0.1266, 0.106, respectively. With regards to the proposed model with Softsign function (i = 4), when the excitation level is 0-60-0 V and 70 Hz, although the values of RMSE, MAPE and SMAPE of the proposed model with Softsign function (i = 4) are 0.1076, 0.0307 and 0.0368, the difference is acceptable, only 60.96%, 48.76% and 75.49% higher than the lowest values in the other four proposed models. In summary, although the five proposed models can all fit the measured displacement-voltage hysteresis loop well, the overall fitting performance of the proposed model

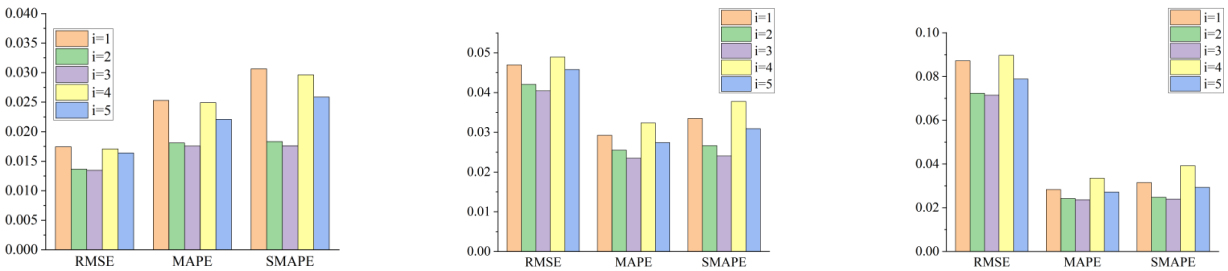

(a) 0-20-0 V (b) 0-40-0 V (c) 0-60-0 V

Fig. 8 Comparison of evaluation metrics among the proposed five models for 20 Hz frequency case

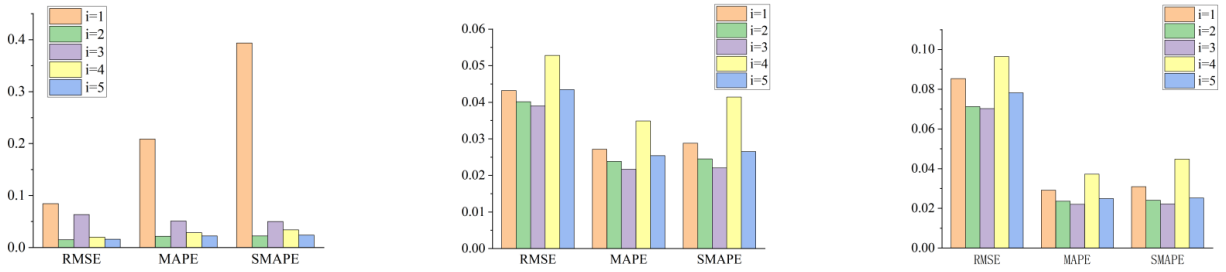

(a) 0-20-0 V (b) 0-40-0 V (c) 0-60-0 V

Fig. 9 Comparison of evaluation metrics among the proposed five models for 40 Hz frequency case

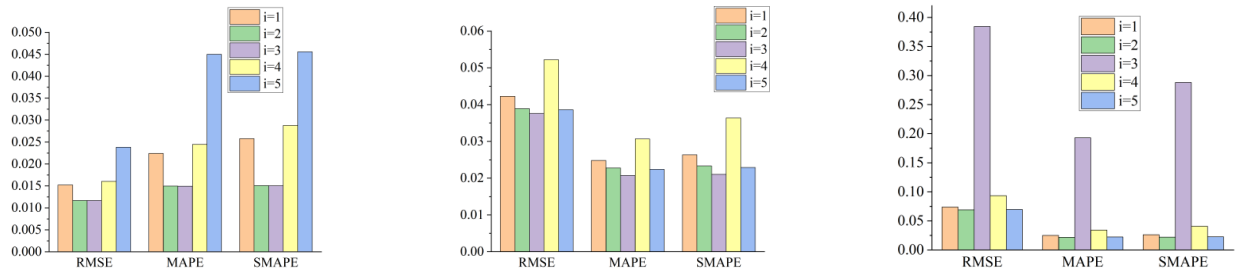

(a) 0-20-0 V (b) 0-40-0 V (c) 0-60-0 V

Fig. 10 Comparison of evaluation metrics among the proposed five models for 60 Hz frequency case

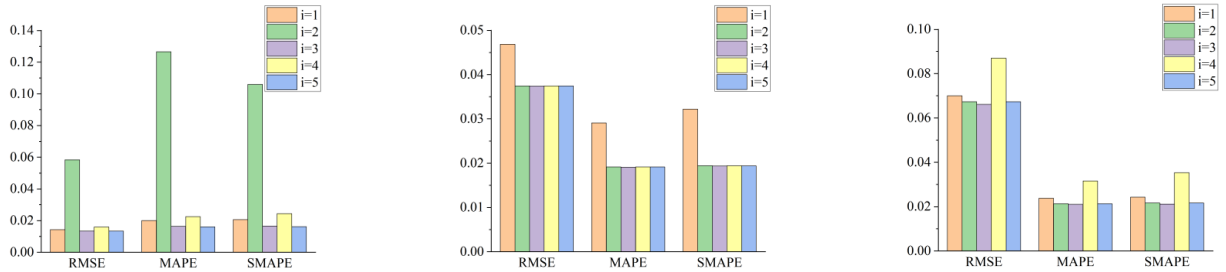

(a) 0-20-0 V (b) 0-40-0 V (c) 0-60-0 V

Fig. 11 Comparison of evaluation metrics among the proposed five models for 80 Hz frequency case

with Softsign function (i = 4) is the most stable among the five proposed models, based on the performance parameters of RMSE, MAPE and SMAPE.

In addition, the operation efficiency (running time of a single simulation) of the five proposed models is also studied. The following table shows the operation efficiency of 0-20-0 V, 0-40-0 V and 0-60-0 V respectively under the loading condition of 40 Hz. The results show that there is no significant difference among the five proposed models. All the running time of the five proposed models are acceptable.

Based on the analysis above, the overall fitting performance of the proposed model with Sigmoid function (i = 4) outperform the other four models, with terms of stability. And its computation efficiency doesn't show significant disadvantage compared with the other models.

In brief, it is well acknowledged that highly nonlinear differential equations will cause a large amount of computation and introduce fitting errors, threatening the simulation accuracy. Apparently, in the proposed model, an element based on activation function is employed to replace

Table 7 Comparison of running time among the five proposed models under 40 Hz

Model	i = 1	i = 2	i = 3	i = 4	i = 5
Time (s) (0-20-0 V)	72.5312	81.8668	60.6915	74.6415	52.5113
Time (s) (0-40-0 V)	60.665	68.8223	67.7509	76.7814	71.8077
Time (s) (0-60-0 V)	58.255	83.8631	79.9322	53.2539	62.845

nonlinear differential equations in BW model. Through replacing the nonlinear differential equation with activation function, the proposed model features less undetermined parameters and computation, and avoids the errors caused by dealing with nonlinear differential equations.

The proposed models also provide feasible choice for engineering application. Feedback control and open-loop control are two major methods to guarantee positioning precision in engineering. Feedback control can reduce

positioning errors and achieve high positioning accuracy in many PZT application devices. However, it still faces problems such as response speed, stability, oscillation and overshoot, and features complex structure, high cost and troublesome design. Then open-loop control based on precise hysteresis model become a good choice. Although it can't completely eliminate the positioning error, but can effectively reduce the positioning error and expedite the response speed of the system, while keeping the cost low. Especially, the combination of the feedback control and open-control can improve the response speed and stability of the system on the basis of eliminating the positioning error.

5. Conclusions

In this paper, five hysteresis models based on activation function are proposed to characterize the nonlinear displacement-voltage response of PZT actuators. Compared with the standard BW model, the proposed five models feature fewer parameters and no nonlinear differential equation in the expression, and have the advantage of high calculation accuracy. The performance of the proposed five models is verified through the experimental data and PSO algorithm. In addition, the comparison performance of the five models is made and specific recommendation is given. The detailed conclusions are drawn as follows.

- The five proposed hysteresis models are effective in depicting hysteresis displacement-voltage responses of PZT actuators with high accuracy.
- The five proposed hysteresis models are comprehensively superior to standard BW model in modelling the nonlinear hysteresis displacement-voltage responses, in terms of hysteresis loop smoothness and prediction error.
- The proposed model with Softsign function (i = 4) outperforms the other proposed models, considering stability performance.

Acknowledgments

This research is supported by the National Natural Science Foundation of China (No. U23A20618, No. 52075273) and Ningbo Science and Technology Innovation 2025 Major Project (No.2020Z070).

References

Al Janaideh, M., Rakotondrabe, M. and Aljanaideh, O. (2016), "Further results on hysteresis compensation of smart micropositioning systems with the inverse Prandtl-Ishlinskii compensator", *IEEE Transact. Control Syst. Technol.*, **24**(2), 428-439. https://doi.org/10.1109/TCST.2015.2446959

Ali, H.I., Noor, S.B.M. and Marhaban, M.H. (2010), "PSO-based robust H-infinity controller design using cascade compensation network", *IEICE Electron. Expr.*, **7**(12), 832-838. https://doi.org/10.1587/elex.7.832

Ali, A., Pasha, R.A., Elahi, H., Sheeraz, M.A., Bibi, S., Hassan, Z.U., Eugeni, M. and Gaudenzi, P. (2019), "Investigation of deformation in bimorph piezoelectric actuator: analytical, numerical and experimental approach", *Integr. Ferroelectr.*, **201**(1), 94-109. https://doi.org/10.1080/10584587.2019.1668694

Aziz, N.A.A., Ibrahim, Z., Mubin, M., Nawawi, S.W. and Mohamad, M.S. (2018), "Improving particle swarm optimization via adaptive switching asynchronous-synchronous update", *Appl. Soft Comput.*, **72**, 298-311. https://doi.org/10.1016/j.asoc.2018.07.047

Baziyad, A.G., Ahmad, I., Salamah, Y.B. and Alkuhayli, A. (2022), "Robust tracking control of piezo-actuated nanopositioning stage using improved inverse LSSVM hysteresis model and RST controller", *Actuators*, **11**(11), 324. https://doi.org/10.3390/act11110324

Das, S. and Dhang, N. (2020), "Structural damage identification of truss structures using self-controlled multi-stage particle swarm optimization", *Smart Struct. Syst., Int. J.*, **25**(3), 345-368. https://doi.org/10.12989/sss.2020.25.3.345

Feng, Y. and Li, Y. (2021), "System identification of micro piezoelectric actuators via rate-dependent prandtl-ishlinskii hysteresis model based on a modified PSO algorithm", *IEEE Transact. Nanotechnol.*, **20**, 205-214. https://doi.org/10.1109/TNANO.2020.3034965

Fung, R.F., Han, C.F. and Chang, J.R. (2008), "Dynamic modeling of a high-precision self-moving stage with various frictional models", *Appl. Math. Model.*, **32**(9), 1769-1780. https://doi.org/10.1016/j.apm.2007.06.012

Gan, J. and Zhang, X. (2019), "Nonlinear hysteresis modeling of piezoelectric actuators using a generalized Bouc–Wen model", *Micromachines-basel.*, **10**, 183. https://doi.org/10.3390/mi10030183

Gan, J., Mei, Z., Chen, X., Zhou, Y. and Ge, M.F. (2019), "A modified Duhem model for rate-dependent hysteresis behaviors", *Micromachines-basel*, **10**(10), 680. https://doi.org/10.3390/mi10100680

Guo, P., Guan, X. and Ou, J. (2014), "Physical modeling and design method of the hysteretic behavior of magnetorheological dampers", *J. Intel. Mat. Syst. Struct.*, **25**(6), 680-696. https://doi.org/10.1177/1045389X13500576

Huang, H.W., Liu, T.T. and Sun, L.M. (2019), "Multi-mode cable vibration control using MR damper based on nonlinear modeling", *Smart Struct. Syst., Int. J.*, **23**(6), 565-577. https://doi.org/10.12989/sss.2019.23.6.565

Ionescu, F., Konstadinov, K., Arghir, S. and Arotaritei, D. (2011), "Hybrid micro-nano robot for cell and cristal manipulations", *J. Control Eng. Appl. Inform.*, **13**(2), 56-63. https://doi.org/2011-06-18

Ji, H., Lv, B., Ding, H., Yang, F., Qi, A., Wu, X. and Ni, J. (2022), "Modeling and control of hysteresis characteristics of piezoelectric micro-positioning platform based on Duhem Model", *Actuators*, **11**(5), 122. https://doi.org/10.3390/act11050122

Jung, J. and Huh, K. (2010), "Simulation tool design for the two-axis nano stage of lithography systems", *Mechatronics*, **20**(5), 574-581. https://doi.org/10.1016/j.mechatronics.2010.06.003

Kenton, B.J., Fleming, A.J. and Leang, K.K. (2011), "Compact ultra-fast vertical nanopositioner for improving scanning probe microscope scan speed", *Rev. Sci. Instrum.*, **82**(12), 123703. https://doi.org/10.1063/1.3664613

Kim, K., Nilsen, E., Huang, T., Kim, A., Ellis, M., Skidmore, G. and Lee, J.B. (2004), "Metallic microgripper with SU-8 adaptor as end-effectors for heterogeneous micro/nano assembly applications", *Microsyst. Technol.*, **10**(10), 689-693. https://doi.org/10.1007/s00542-004-0367-6

Li, Y., Zhu, J., Li, Y. and Zhu, L. (2022), "A hybrid Jiles–Atherton and Preisach model of dynamic magnetic hysteresis based on backpropagation neural networks", *J. Magn. Magn. Mater.*, **544**,

168655. https://doi.org/10.1016/j.jmmm.2021.168655

Liu, C.H., Jywe, W.Y., Jeng, Y.R., Hsu, T.H. and Li, Y.T. (2010), "Design and control of a long-traveling nano-positioning stage", *Precis. Eng.*, **34**(3), 497-506. https://doi.org/10.1016/j.precisioneng.2010.01.003

Liu, Y., Du, D., Qi, N. and Zhao, J. (2019), "A distributed parameter Maxwell-slip model for the hysteresis in piezoelectric actuators", *IEEE Transact. Indust. Electron.*, **66**, 7150-7158. http://doi.org/10.1002/abio.370040210

Liu, Y.F., Wang, Y. and Chen, X. (2020), "Online hysteresis identification and compensation for piezoelectric actuators", *IEEE Transact. Indust. Electron.*, **67**(7), 5595-5603. https://doi.org/10.1109/TIE.2019.2934022

Liu, Y., Ni, C., Du, D. and Qi, N. (2021), "Learning piezoelectric actuator dynamics using a hybrid model based on Maxwell-Slip and Gaussian processes", *IEEE-ASME Transact. Mechatron.*, **27**(2), 725-732. https://doi.org/10.1109/TMECH.2021.3070187

Luo, Y., Qu, Y., Zhang, Y., Xu, M., Xie, S. and Zhang, X. (2019), "Hysteretic modeling and simulation of a bilateral piezoelectric stack actuator based on Preisach model", *Int. J. Appl. Electrom.*, **59**, 271-280. http://doi.org/10.3233/JAE-171251

Mittal, S. and Meng, C.H. (2000), "Hysteresis compensation in electromagnetic actuators through Preisach model inversion", *IEEE-ASME Transact. Mechatron.*, **5**(4), 394-409. https://doi.org/10.1109/3516.891051

Muftah, M.N., Faudzi, A.A.M., Sahlan, S. and Shouran, M. (2022), "Modeling and fuzzy fopid controller tuned by PSO for pneumatic positioning system", *Energies*, **15**(10), 3757. https://doi.org/ 10.3390/en15103757

Nguyen, P.B., Choi, S.B. and Song, B.K. (2018), "A new approach to hysteresis modelling for a piezoelectric actuator using Preisach model and recursive method with an application to open-loop position tracking control", *Sensor Actuat. A-Phys.*, **270**, 136-152. https://doi.org/10.1016/j.sna.2017.12.034

Nguyen-Ngoc, L., Tran, N.H., Bui-Tien, T., Mai-Duc, A., Abdel Wahab, M., X Nguyen, H. and De Roeck, G. (2021), "Damage detection in structures using particle swarm optimization combined with artificial neural network", *Smart Struct. Syst., Int. J.*, **28**(1), 1-12. https://doi.org/10.12989/sss.2021.28.1.001

Pasco, Y. and Berry, A. (2004), "A hybrid analytical/numerical model of piezoelectric stack actuators using a macroscopic nonlinear theory of ferroelectricity and a preisach model of hysteresis", *J. Intel. Mat. Syst. Struct.*, **15**(5), 375-386. https://doi.org/10.1177/1045389X04040907

Qian, C., Ouyang, Q., Song, Y. and Zhao, W. (2020), "Hysteresis modeling of piezoelectric actuators with the frequency-dependeng behavior using a hybrid model", *Proceedings of the Institution of Mechanical Engineers, Part C: J. Mech. Eng. Sci.*, **234**(9), 1848-1858. https://doi.org/10.1177/0954406219897089

Rakotondrabe, M. (2017), "Multivariable classical Prandtl-Ishlinskii hysteresis modeling and compensation and sensorless control of a nonlinear 2-dof piezoactuator", *Nonlinear Dyn.*, **89**(1), 481-499. https://doi.org/10.1007/s11071-017-3466-5

Savoie, M. and Shan, J.J. (2022), "Temperature-dependent asymmetric Prandtl-Ishlinskii hysteresis model for piezoelectric actuators", *Smart Mater. Struct.*, **31**(5), 055022. https://doi.org/10.1088/1361-665X/ac6552

Schweizer, B. (2017), "Hysteresis in porous media: Modelling and analysis", *Interface Free Bound.*, **9**(3), 417-447. https://doi.org/ 10.4171/IFB/388

Sente, P.A., Labrique, F.M. and Alexandre, P.J. (2011), "Efficient control of a piezoelectric linear actuator embedded into a servo-valve for aeronautic applications", *IEEE Transact. Indust. Electron.*, **59**(4), 1971-1979. https://doi.org/10.1109/TIE.2011.2165450

Sherrit, S., Bao, X., Jones, C.M., Aldrich, J.B., Blodget, C.J., Moore, J.D., Carson, J.W. and Goullioud, R. (2011), "Piezoelectric multilayer actuator life test", *IEEE Transact. Ultrason. Ferroelect. Freq. Control*, **58**(4), 820-828. https://doi.org/10.1109/TUFFC.2011.1874

Shome, S.K., Mukherjee, A., Karmakar, P. and Datta, U. (2018), "Adaptive feed-forward controller of piezoelectric actuator for micro/nano-positioning", *Sādhanā.*, **43**(10), 158. https://10.1007/s12046-018-0925-8

Tang, H., Zhang, W., Xie, L. and Xue, S. (2013), "Multi-stage approach for structural damage identification using Particle Swarm Optimization", *Smart Struct. Syst., Int. J.*, **11**(1), 69-86. https://doi.org/10.12989/sss.2013.11.1.069

Tao, G. and Kokotovic, P.V. (1995), "Adaptive control of plants with unknown hystereses", *IEEE Transact. Automat. Control*, **40**(2), 200-212. https://doi.org/10.1109/9.341778

Tue, P.T., Shimura, R., Shimoda, T. and Takamura, Y. (2019), "Direct integration of piezoactuators array with active-matrix oxide thin-flim transistors using a low-temperature solution process", *Sensor Actuat. A-Phys.*, **295**(15), 125-132. https://doi.org/10.1016/j.sna.2019.04.040

Vorbringer-Dorozhovets, N., Hausotte, T., Manske, E., Shen, J.C. and Jäger, G. (2011), "Novel control scheme for a high-speed metrological scanning probe microscope", *Meas. Sci. Technol.*, **22**(9), 094012. https://doi.org/10.1088/0957-0233/22/9/094012

Wang, D. and Zhu, W. (2011), "A phenomenological model for pre-stressed piezoelectric ceramic stack actuators", *Smart Mater. Struct.*, **20**, 035018. https://doi.org/10.1088/0964-1726/2/3/035018

Xiao, S. and Li, Y. (2012), "Modeling and high dynamic compensating the rate-dependent hysteresis of piezoelectric actuators via a novel modified inverse Preisach model", *IEEE Transact. Control Syst. Technol.*, **21**, 1549-1557. https://doi.org/10.1109/TCST.2012.2206029

Xu, Q. and Li, Y. (2010), "Dahl model-based hysteresis compensation and precise positioning control of an XY parallel micromanipulator with piezoelectric actuation", *J. Dyn. Syst.-t ASME*, **132**(4). https://doi.org/10.1115/1.4001712

Yu, Y., Li, Y.C. and Li, J.C. (2015), "Parameter identification of a novel strain stiffening model for magnetorheological elastomer base isolator utilizing enhanced particle swarm optimization", *J. Intel. Mat. Syst. Struct.*, **26**(18), 2446-2462. https://doi.org/10.1177/1045389X14556166

Zhang, M. and Damjanovic, D. (2020), "A quasi-Rayleigh model for modeling hysteresis of piezoelectric actuators", *Smart Mater. Struct.*, **29**(7), 075012. https://doi.org/10.1088/1361-665X/ab874b

Zhang, Q., Dong, Y., Peng, Y., Luo, J., Xie, S. and Pu, H. (2019), "Asymmetric Bouc–Wen hysteresis modeling and inverse compensation for piezoelectric actuator via a genetic algorithm–based particle swarm optimization identification algorithm", *J. Intell. Mater. Syst. Struct.*, **30**, 1263-1275. https://doi.org/10.1177/1045389X19831360